1

ULTRAFAST TIME-RESOLVED STUDIES OF THE PHOTOCHEMISTRY OF ARYL AZIDES

JIN WANG, GOTARD BURDZINSKI, AND MATTHEW S. PLATZ

1.1 INTRODUCTION

Kasha's rule states that a photophysical and/or photochemical process originates from the lowest vibrational level of the lowest excited state.[1] This rule is very successful in explaining the commonly observed mirror image symmetry between the vibronic structure of absorption and fluorescence spectra[2] and wavelength-

Nitrenes and Nitrenium Ions, First Edition. Edited by Daniel E. Falvey and Anna D. Gudmundsdottir.

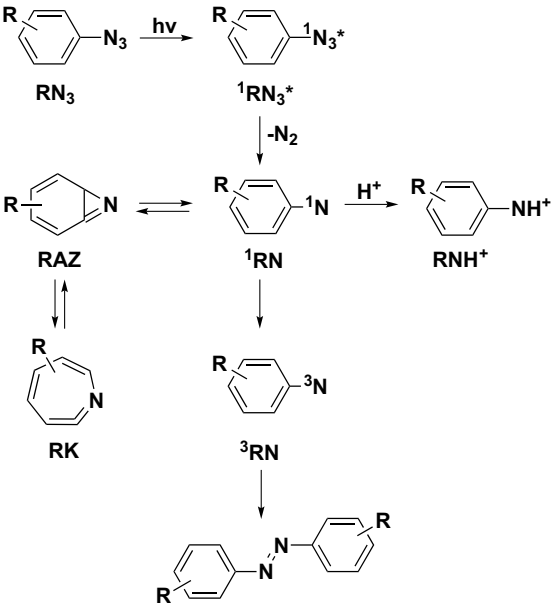

SCHEME 1.1. General reaction pathways for aryl azides.

independent photochemistry.[3] However, exceptions to Kasha's rule are known. A very well-known exception is provided by azulene, whose fluorescence originates from the S_2 state and whose corresponding absorption and emission spectra are not mirror images.[4] Also, numerous photochemical wavelength-dependent reactions are known. For example, the photolysis of diazirines using different excitation wavelengths produces different quantum yields and even different photoproducts.[5,6] Therefore, it is important to understand the nature of the excited state of a photochemical reaction precursor and the competition between all of the pathways by which it can decay.

The photolysis of aromatic azides promotes nitrogen extrusion and the release of singlet nitrenes (Scheme 1.1).[7,8] The chemistry of aryl nitrenes has been extensively studied by chemical, physical, and computational methods.[9,10] The quantum yields of light-induced decomposition of the naphthyl azides are close to unity and that of simple phenyl azides fall in the range 0.1–0.7 and depend on the concentration of the azide.[11–18] To the best of our knowledge, simple phenyl, biphenylyl, and naphthyl azides lack observable fluorescence, which is consistent with their large quantum yields for extrusion of molecular nitrogen. Otherwise, essentially nothing was known of the details by which aryl azide excited states decompose to form singlet nitrenes at the outset of this project. The development of ultrafast spectroscopic techniques and modern quantum chemical computational methods provides tools with which to begin to understand how the excited state surfaces of aryl azides connect to the ground state surfaces of the nitrenes.

Numerous aryl nitrenes have been studied extensively using nanosecond laser flash photolysis (ns-LFP), nanosecond time-resolved infrared (ns-TRIR), matrix isolation spectroscopy and with the tools of computational chemistry. Gritsan and Platz have recently presented a very comprehensive review of this subject.[9] Photolysis of phenyl azide (PhN_3, Scheme 1.1, R = H) leads to the production of singlet phenyl nitrene (^{1}PhN), benzazirine (PhAZ), ketenimine (PhK), and triplet nitrene (^{3}PhN). The lifetime of ^{1}PhN is $\sim$1 ns in organic solvents at ambient temperature, and is controlled by intersystem crossing to its lower-energy triplet state, ^{3}PhN, intramolecular rearrangements and intermolecular acid–base reactions (Scheme 1.1). Some singlet aryl nitrenes have even shorter lifetimes in solution, such as singlet *o*-biphenylyl nitrene and 1- and 2-naphthyl nitrenes, due to their rapid intramolecular rearrangements. These reactive intermediates cannot be observed by nanosecond time-resolved spectroscopies at room temperature. Matrix spectroscopic methods utilize very low temperature to suppress chemical reactions of reactive intermediates, but cannot prevent relaxation by intersystem crossing unless intersystem crossing (ISC) is accompanied by a large geometry change.[19] Most aryl nitrenes have triplet ground states and thus, short-lived singlet aryl nitrenes cannot be characterized by matrix isolation spectroscopic methods. The development of ultrafast time-resolved spectroscopy provides the first opportunity to study these very short-lived reactive intermediates by direct observational techniques.

Nitrenium ions are the conjugate acids of nitrenes. Falvey has reviewed recent developments in the field of nitrenium ion chemistry.[20] McClelland's group pioneered the field of producing nitrenium ions by protonating nitrenes.[21–23] This method works particularly well when the singlet nitrene to be intercepted has a relatively long lifetime (>10 ns) in an aprotic solvent at ambient temperatures. In this manner, *p*-biphenylyl nitrenium cation (*p*-$BpNH^+$), produced by protonation of singlet *p*-biphenylyl nitrene (^{1}*p*-BpN), was readily detected by nanosecond transient UV–Vis spectroscopy.[21–24] Phillips et al. subsequently studied this nitrenium cation in water using time-resolved resonance Raman spectroscopy and assigned the spectra with the aid of density functional theory (DFT) calculations.[25] The intrinsic drawback of McClelland's method is that the protonation of the singlet nitrene has to be very rapid to compete with other deactivation channels, such as intersystem crossing to the lower-energy triplet state, and intramolecular rearrangement. *o*-Biphenylyl nitrene (*o*-BpN) and 1-naphthyl nitrene (1-NpN) are well-known short-lived singlet nitrenes, whose lifetimes in CH_3CN (16 and 12 ps, respectively)[26,27] are controlled by intramolecular cyclizations. Thus, even when protonation can compete with the other decay channels, ultrafast spectroscopic methods will still be required to resolve the formation of these nitrenium cations.

In this chapter, we will describe the application of ultrafast transient absorption spectroscopy in the study of the photochemistry of *para*- and *ortho*-biphenylyl azides (*p*-BpN_3 and *o*-BpN_3, respectively) and 1-naphthyl and 2-naphthyl azides (1-NpN_3 and 2-NpN_3, respectively) and report the observation of the S_2 azide excited states and lifetimes, the spectra and lifetimes of the corresponding singlet aryl nitrenes in acetonitrile solution at ambient temperature and the formation of their corresponding nitrenium ions in protic solvents. This chapter will mainly focus on

experimental results. For a detailed discussion of quantum mechanical calculations on excited states, see Chapter 2 by Hadad et al.

1.2 ARYL AZIDE EXCITED STATES AND NITRENES

1.2.1 Ultrafast UV–Vis Studies

1.2.1.1 p-Biphenylyl and o-Biphenylyl Azides. The photochemistry of aryl azides and their corresponding nitrenes have been reviewed by Gritsan and Platz.[9] We will take *p*-biphenylyl azide (*p*-BpN_3) as an example to briefly illustrate the relevant photochemical pathways (Scheme 1.1, $R = p$-biphenyl). On photolysis of *p*-BpN_3, the initially formed, relaxed, singlet nitrene ^1p-BpN (^{1}RN, R = *p*-biphenyl) has $\lambda_{max} = 343$ nm and $\tau = \sim 9$ ns at ambient temperature.[28] At ambient temperature, the lifetime of ^1p-BpN is controlled by cyclization to benzazirine RAZ. At 77 K, the singlet nitrene undergoes intersystem crossing to its lower-energy triplet spin isomer, ^3p-BpN (^{3}RN, R = *p*-biphenyl) with a rate constant $k_{isc} = (9.3 \pm 0.4) \times 10^6\ s^{-1}$ in 3-methylpentane.[28] The benzazirines derived from most phenyl nitrenes rapidly ring-open at ambient temperature to form 1,2,4,5-azacycloheptatetraenes, RK (Scheme 1.1, also referred to as 1,2-didehydroazepines or cyclic ketenimines, see Section 1.2.2 for a detailed discussion of the formation of RK).[9,10]

Ultrafast laser flash photolysis (LFP) of *p*-BpN_3 ($\lambda_{ex} = 266$ nm) in acetonitrile at ambient temperature produces the transient spectra shown in Figure 1.1a.[26] There is a broadly absorbing transient at 480 nm that forms within the laser pulse and decays within the 300 fs laser pulse (Fig. 1.1a). As transient absorption decays at 480 nm, it grows at 350 nm (Fig. 1.1a). The latter species is readily assigned to ^1p-BpN on the basis of nanosecond time-resolved studies.[28] The precursor of the singlet aryl nitrene is assigned to an excited state of azide ^1p-$BpN_3{}^*$ which absorbs at 480 nm.

Similarly, ultrafast LFP ($\lambda_{ex} = 266$ nm) of *ortho*-biphenylyl azide (*o*-BpN_3) in acetonitrile at ambient temperature produces a transient absorption at 480 nm, which is formed within the laser pulse and decays with a time constant of 450 ± 150 fs (Fig. 1.2a). As this absorption decays, a new absorption at 400 nm (^1o-BpN) grows with an isosbestic point at 435 nm and a time constant of 280 ± 150 fs, the same time constant as the decay of ^1o-$BpN_3{}^*$ within experimental error.

Hackett and Hadad's calculations predict that the transition of S_0 to S_2 has a much larger oscillator strength than the S_0 to S_1 transition in all of the aromatic azides considered in this chapter (see Chapter 2 for details).[26] Thus, UV excitation of the biphenylyl and naphthyl azides is predicted to promote the ground state of the azide to the S_2 state. The S_2 state will deactivate rapidly through internal conversion to the S_1 state of the aromatic azides. The S_1 state of the azide is predicted to undergo nitrogen extrusion over a small barrier of $\sim$2 kcal/mol. This process is highly exothermic (typically by $\sim$40 kcal/mol) and a vibrationally excited nitrene will be formed. The S_1 state of the azide may also deactivate to reform the ground state, thereby reducing the efficiency of aryl nitrene formation. Thus, the initially detected transients in studies of the photochemistry of *p*-BpN_3 and *o*-BpN_3 are assigned to the

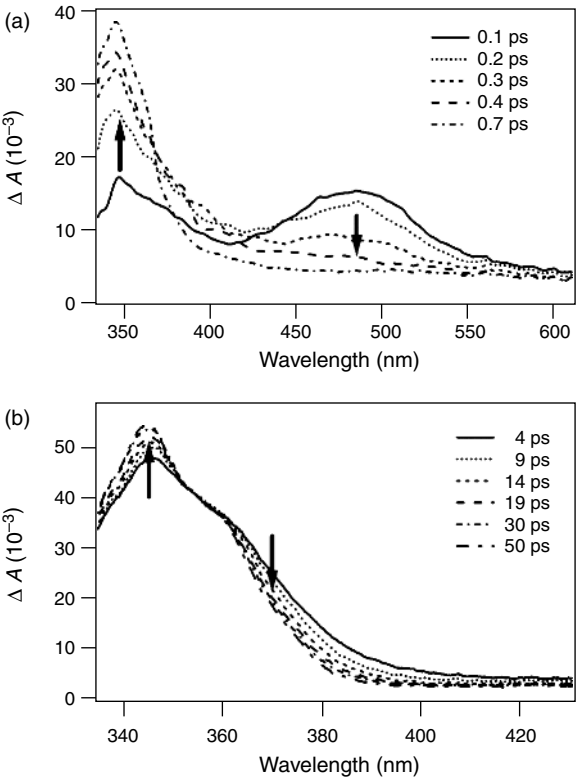

FIGURE 1.1. Transient absorption spectra produced by 266 nm photolysis of *p*-biphenylyl azide in acetonitrile at ambient temperature with time windows of (a) 0.1–0.7 ps and (b) 4–50 ps. *Source*: Reprinted with permission from Ref. 26.

S_2 states of the azides on the basis of Hackett and Hadad's calculations for the oscillator strengths and necessary excitation energies.[26]

Our studies of a series of biphenylyl diazo compounds reveal similar excited states which absorb between 470 and 500 nm and their lifetimes are all within the instrument response (300 fs).[29–35] Hackett and Hadad's calculations show that the electron densities of the S_2 excited states of *p*- and *o*-biphenylyl azides are localized on the biphenyl ring. Although the corresponding computational results of the biphenylyl diazo compounds are unavailable, it is reasonable to predict that on UV photolysis, the electron densities of the excited states (presumably the S_2 excited states) of the biphenylyl diazo compounds are also localized on the biphenyl rings. Thus, similar excited states can be observed for biphenylyl azides and biphenylyl diazo compounds. Ultrafast photolysis ($\lambda_{ex} = 270$ nm) of biphenyl in acetonitrile also produces an excited state centered at 470 nm (unpublished results), which confirms that the excited states observed for *p*- and *o*-BpN_3 are localized on the biphenyl ring.

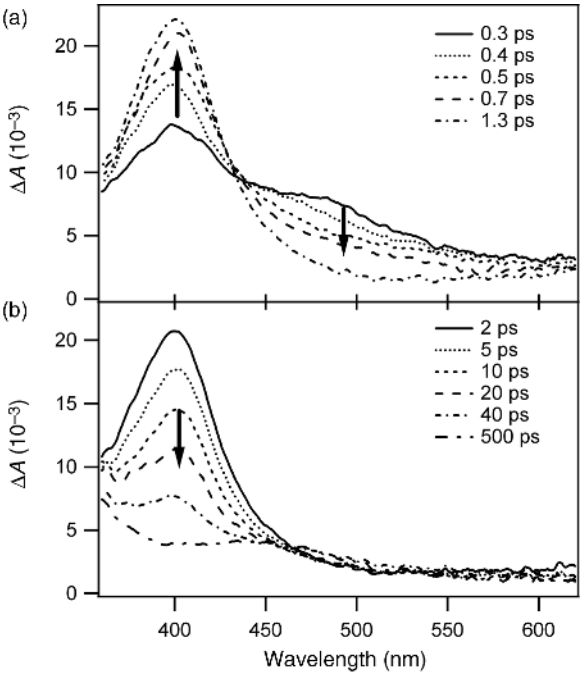

FIGURE 1.2. Transient absorption spectra produced by 266 nm photolysis of *o*-biphenylyl azide in acetonitrile at ambient temperature with time windows of (a) 0.3–1.3 ps and (b) 2–500 ps. *Source*: Reprinted with permission from Ref. 26.

As expected, relaxed singlet nitrene ^1p-BpN does not exhibit any significant population decay on the 100 ps timescale ($\tau \sim 9$ ns).[28] However, the transient absorption spectrum of the initially formed singlet nitrene (^1p-BpN) undergoes vibrational cooling (VC)[36–39] (Fig. 1.1b), which manifests as a decay on the red edge (380 nm) and a rise on the blue edge (345 nm) of the absorption band with the same time constant ($\tau = 11$ ps). The time-dependent band narrowing is characteristic of vibrational cooling of species initially formed with excess vibrational energy. A derivative of ^1o-BpN, 3,5-dichloro-*ortho*-biphenyl nitrene also undergoes vibrational cooling in cyclohexane with a time constant of 11 ps.[40] Furthermore, in a related ultrafast study of 2-fluorenyl azide, a similar spectral evolution was also observed.[41] This rules out the possibility that the spectral changes are due to rotation around the C—C bond of the biphenyl moiety.

^1o-BpN decays with a time constant of 16 ± 3 ps (Fig. 1.2b). The 16 ps time constant represents the population decay of the singlet nitrene (^1o-BpN) by isomerization to both isocarbazole and a benzazirine (and subsequently the benzazirine ring expands to form a 1,2-didehydroazepine, Scheme 1.2). The spectrum of ^1o-BpN does not undergo reshaping characteristic of vibrational cooling, even though the decay of ^1o-BpN takes place on the timescale of vibrational cooling.

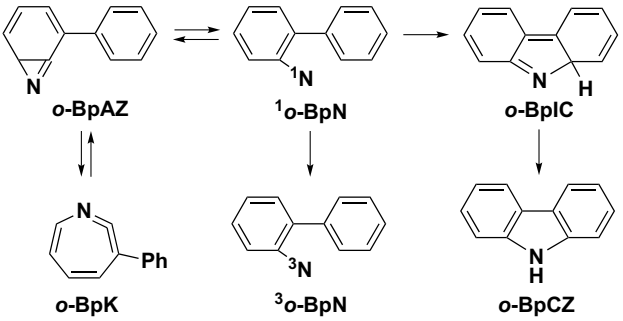

SCHEME 1.2. Reaction pathways for *o*-biphenylyl azide.

Thus, either ^1o-BpN is formed vibrationally relaxed, or, most likely, we are monitoring the disappearance of ^1o-BpN before it can completely shed its excess heat to solvent. The Sundberg group discovered that the formation rate of benzazirine k_{az} is comparable to that of isocarbazole k_{car} based on diethylamine trapping experiments.[42,43] Assuming k_{az} equals to k_{car}, one can deduce that $k_{az} = k_{car} = 3.1 \times 10^{10}\,s^{-1}$ based on $k_{obs} = k_{az} + k_{car} = 1/(16\,ps)$. Furthermore, assuming that the pre-exponential factors for both reactions are $10^{13}\,s^{-1}$, their activation energies can be deduced as ~3.4 kcal/mol. The Borden group[28] calculated the activation barriers for the formation of benzarine and isocarbozole from ^1o-BpN are 6.8 and 6.0 kcal/mol, respectively, which are overestimated by ~3 kcal/mol based on previous experience with open shell systems. Their calculations also showed that the activation barrier of benzazirine formation for ^1o-BpN is 3.2 kcal/mol lower than that for parent phenyl nitrene. Using the experimentally measured value of 5.6 kcal/mol for benzazirine formation from phenyl nitrene as a benchmark, they estimated a barrier of 2.4 kcal/mol for ^1o-BpN cyclization, which is in good agreement with our previous analysis (~3.4 kcal/mol).

At room temperature, the decay of ^1p-BpN is mainly controlled by formation of benzazirine. Based on the lifetime of ^1p-BpN of ~9 ns in acetonitrile at 298 K, the benzarine formation rate for ^1p-BpN is $1.1 \times 10^8\,s^{-1}$, which is substantially slower than that for ^1o-BpN ($3.1 \times 10^{10}\,s^{-1}$). The faster reaction for ^1o-BpN is mainly due to relief of the steric interaction between the nitrogen and the *ortho*-hydrogen atoms. The dihedral angles for ^1p-BpN and ^1o-BpN are 33.1° and 44.4°, respectively.[281] o-BpN enjoys less conjugation between the two phenyl rings and is less stable than ^1p-BpN. Thus, the benzarine formation activation barrier for ^1o-BpN will be smaller than that for ^1p-BpN due to the destabilization of the reactant (Scheme 1.3).

1.2.1.2 1-Naphthyl and 2-Naphthyl Azides. The photochemistry of 1-naphthyl azide (1-NpN_3) has been studied by chemical,[44–49] physical,[50–52] and computational methods.[52,53] Ultrafast LFP ($\lambda_{ex} = 266$ nm) of 1-NpN_3 in acetonitrile produces the transient spectra of Figure 1.3.[26] The transient absorption band centered at 460 nm is formed within the time resolution of the spectrometer (300 fs). We attribute the transient absorption spectrum observed at 460 nm at early delay times to the S_2 state

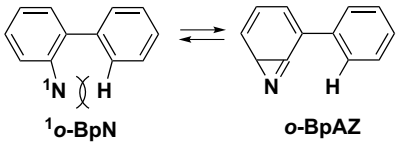

SCHEME 1.3. Steric interaction in *o*-biphenylyl nitrene.

of 1-NpN_3 based on Hackett's calculations. This excited state species decays with a time constant of 730 fs (Fig. 1.3a). As in the case of the biphenylyl azides, the absorption maximum of the excited azide S_2 ($\pi \rightarrow (\pi^*$,aryl)) of 1-NpN_3 is not far from the S_1 ($\pi \rightarrow \pi^*$) absorption maximum of naphthalene.

At longer delay times (>3 ps), only the 385 nm band is observed. The carrier of this species can be assigned with confidence to the absorption of ^{1}1-NpN, as this species had been previously observed by nanosecond time-resolved LFP of 1-NpN_3 at 77 K.[53] The transient absorption of ^{1}1-NpN monitored at 385 nm decays with a time constant of 12 ps (Fig. 1.3b) at ambient temperature to form naphthazirine (1-NpAZ). 1-NpAZ absorbs strongly below 300 nm and cannot be detected in this

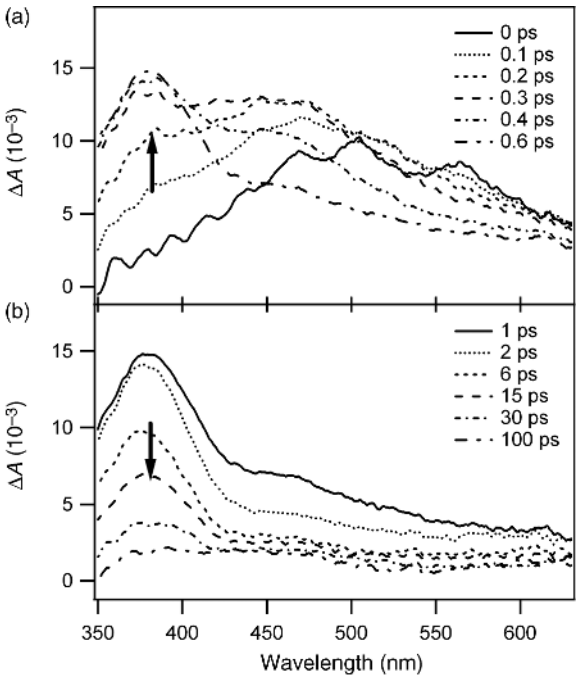

FIGURE 1.3. Transient absorption spectra produced by 266 nm photolysis of 1-naphthyl azide in acetonitrile at ambient temperature with time windows of (a) 0–0.6 ps and (b) 1–100 ps. *Source*: Reprinted with permission from Ref. 26.

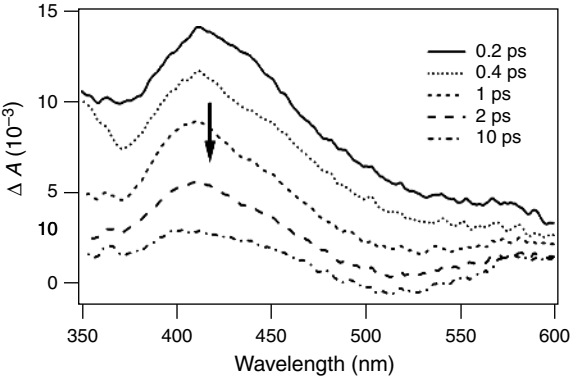

FIGURE 1.4. Transient absorption spectra produced by 266 nm photolysis of 2-naphthyl azide in acetonitrile at ambient temperature with a time window of 0.2–10 ps. *Source*: Reprinted with permission from Ref. 54.

study as the absorption maximum is outside the spectral probe range of 350–620 nm. As in the case of ^{1}*o*-BpN, evidence of vibrational cooling of ^{1}1-NpN is not present. Thus, either ^{1}1-NpN is formed thermally relaxed or it is formed vibrationally excited and isomerizes to naphthazirine (1-NpAZ) at the same or a faster rate that it undergoes vibrational relaxation. Deuteration of the solvent has no discernable influence on the observed dynamics ($\lambda_{ex} = 270$ nm, $\tau_1 = 0.8$ ps, $\tau_2 = 15$ ps).

The spectral analysis of 2-NpN_3 is much more complicated than that of 1-NpN_3. Ultrafast LFP ($\lambda_{ex} = 266$ nm) of 2-naphthyl azide (2-NpN_3) in acetonitrile produces the transient spectrum of Figure 1.4.[54] Transient absorption bands centered at 350 and 420 nm are formed within the time resolution of the spectrometer (300 fs). At longer delay times (>1 ps), only transient absorption at 420 nm is observed. The carrier of the 350 nm band has a shorter lifetime than that of the 420 nm peak, thus we must be detecting the transient absorption of at least two distinct species whose spectra overlap severely. The lifetime of the species absorbing at 420 nm is 1.8 ps (the long-lived component in Fig. 1.5). The lifetime of the carrier of the 350 nm transient absorption is within the instrument response (300 fs, the short-lived component in Fig. 1.5). Similar time constants were obtained in methanol. In this case, theory cannot confidently assign the transient spectra.[53]

Tsao and Platz have extensively studied *ortho,ortho′*-disubstituted phenyl nitrenes and found that the rate of cyclization of a di-*ortho*-substituted singlet aryl nitrene can be retarded by a steric effect.[55] A similar effect was also observed for singlet 3,5-dichloro-*ortho*-biphenylyl nitrene.[40] These *ortho* modifications of aryl nitrenes do not dramatically alter the spectral position of the absorption band. [40,55] For reasons of synthetic convenience, 1-chloro-2-naphthyl azide (Cl-2-NpN_3) was prepared and studied by ultrafast time-resolved spectroscopic techniques (Scheme 1.4) in order to assign the spectral band of ^{1}2-NpN.[54]

Ultrafast photolysis ($\lambda_{ex} = 308$ nm) of 1-chloro-2-naphthyl azide (Cl-2-NpN_3) in methanol produces the transient spectrum shown in Figure 1.6. There is a small weak

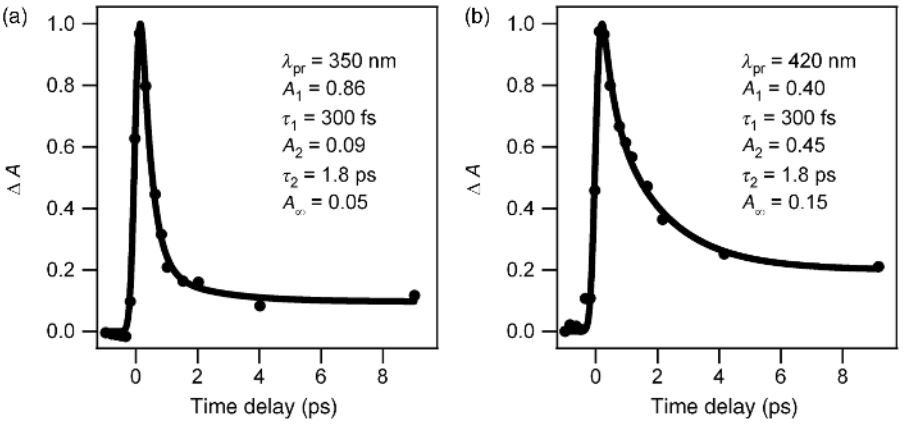

FIGURE 1.5. Normalized kinetic traces of photolysis ($\lambda_{ex} = 266$ nm) of 2-naphthyl azide in acetonitrile at ambient temperature. The kinetic traces are probed at (a) 350 nm and (b) 420 nm and globally fitted in bi-exponential functions with deconvolution of instrument response function (300 fs). *Source*: Reprinted with permission from Ref. 54.

absorption band present at 370 nm and a more intense band is detected at 420 nm with a shoulder at ∼520 nm. The decay of transient absorption at 370 and 520 nm results in a growth of transient absorption at 420 nm, with isosbestic points at 380 and 460 nm (Fig. 1.6a). The latter bands narrow over 5 ps (Fig. 1.6b), as a result of vibrational cooling and then decay over hundreds of picoseconds. Transient absorption at 520 nm is still present after the vibrational cooling is complete. As the 1-chloro substituent is expected to lengthen only the nitrene lifetime, we assign the carriers of the 420 and 520 nm (Fig. 1.6c) transient absorption to singlet 1-chloro-2-

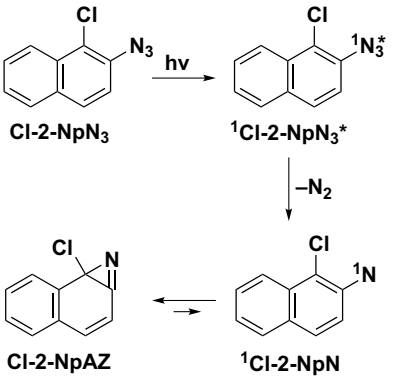

SCHEME 1.4. Reaction pathways for 1-chloro-2-naphthyl azide.

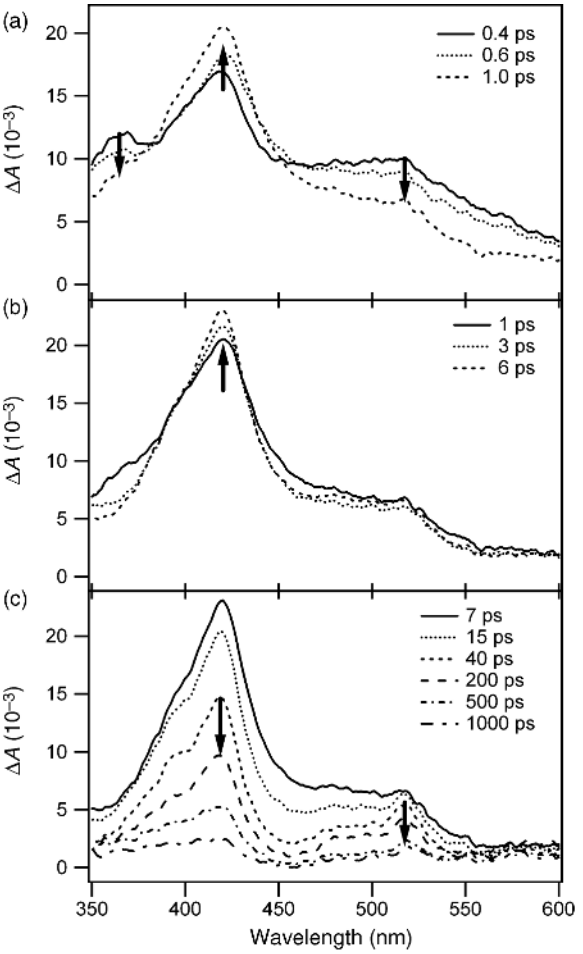

FIGURE 1.6. Transient absorption spectra produced by 308 nm photolysis of 1-chloro-2-naphthyl azide in methanol at ambient temperature. The transient spectra were recorded over time windows of (a) 0.4–1.0 ps (b) 1–6 ps, and (c) 7–1000 ps. *Source*: Reprinted with permission, from Ref. 54.

naphthyl nitrene (^{1}Cl-2-NpN) and by extension, we assign the carrier of 420 nm absorption in Figure 1.4 to singlet 2-naphthyl nitrene. This species (^{1}2-NpN) is the shortest-lived nitrene yet observed ($\tau = 1.8$ ps). The excited state of the azide ^{1}Cl-2-$NpN_3{}^*$ likely has some absorbance at 370 and 520 nm which accounts for the fast (fs) decay component observed at these wavelengths.

Theory predicts that the cyclization of singlet 2-naphthyl nitrene ^{1}2-NpN to naphthazirine 2-NpAZ involves a much lower barrier than the corresponding reaction of singlet 1-naphthyl nitrene (3.02 vs. 5.53 kcal/mol).[52] In fact, nanosecond LFP of 2-naphthyl azide at 77 K *fails* to provide any evidence for the existence of

^{1}2-NpN, unlike the case with singlet 1-naphthyl nitrene,[26] suggesting a picoseconds lifetime or shorter for ^{1}2-NpN, even at 77 K.[53] ^{1}2-NpN must cyclize with a rate constant $\gg 1.1 \times 10^7\ s^{-1}$ at 77 K. Assuming a normal Arrhenius pre-exponential A factor of $10^{13}\ s^{-1}$ for cyclization, one concludes that the barrier to isomerization of ^{1}2-NpN must be less than 2.1 kcal/mol.[53]

1.2.1.3 Phenyl Azide. The chemistry, kinetics, and spectroscopy of phenyl nitrene have been extensively reviewed previously[9] and in this section, we will focus mainly on the excited state of phenyl azide. Phenyl azide (PhN_3) is a convenient light-activated precursor of singlet phenyl nitrene (^{1}PhN).[9] Unfortunately, it is well-documented that on photolysis of PhN_3 in acetonitrile or cyclohexane, a polymeric tar is formed. In an ultrafast time-resolved experiments, tar can form on the surface of the flow cell and prevent spectroscopic analysis under certain conditions.[56] The tar is mainly formed by polymerization of the cyclic ketenimine (Scheme 1.1, K), which is produced by cyclization of ^{1}PhN and subsequent rearrangement of benzazirine (BA). Wirz's group managed to perform ultrafast studies on phenyl azide in dichloromethane (DCM), a solvent which may help to dissolve the polymeric tar to an extent, and reported that the excited state lifetime of phenyl azide is 100 ps.[56] Due to solvent absorption, we could not use DCM as solvent and could not attempt to repeat Wirz's experiment with an excitation wavelength of 270 nm. However, we were able to repeat this experiment in acetonitrile (ACN) containing 1 M diethylamine to scavenge ketenimine K and prevent tar formation.[57] Although this experiment suffers from two-photon absorption by the solvent mixture (with related solvent artifacts for the first few picoseconds after the laser pulse), it is clear that no transient absorption forms several picoseconds after electronic excitation of phenyl azide in ACN containing diethylamine. We also find that the lifetime of the excited state of phenyl azide is $\sim$1 ps, which is significantly shorter than that reported by Wirz et al.

In Section 1.3, we will note that aryl nitrenes protonate efficiently in 88% formic acid and that two very short-lived nitrenes, *o*-biphenylyl nitrene and 1-naphthyl nitrene, can be protonated in this solvent as well to form their corresponding nitrenium ions (see Section 1.2). Taking advantage of formic acid, an excellent nitrene trap, we avoided tar formation and were able to study the photochemistry of phenyl azide using ultrafast spectroscopic methods.[57] In 100% formic acid, the excited state of phenyl azide decays within our instrument response function (300 fs) and a growth below 400 nm is observed, which is assigned to singlet phenyl nitrene (^{1}PhN). This assignment is consistent with the singlet nitrene spectrum reported previously. Based on our ultrafast time-resolved studies of phenyl azide in acetonitrile with diethylamine and in formic acid, we conclude the lifetime of phenyl azide singlet excited state is no longer than 1 ps, similar to its biphenylyl and naphthyl counterparts (Table 1.1).

1.2.2 Ultrafast IR Studies

Ultrafast time-resolved vibrational spectroscopy has the potential for monitoring the dynamics of intermediates involved in photochemistry and providing structural

TABLE 1.1. Summary of Lifetimes and Absorption Maxima of Aryl Azide Singlet Excited States, Singlet Aryl Nitrenes, and Arylnitrenium Ions

	^{1}R —N$_3$*[a]		^{1}R —N[a]		R—NH$^+$[b]		
R = [e]	λ (nm)	τ (fs)	λ (nm)	τ (ps)	λ (nm)	τ_{grow} (ps)	τ_{decay} (ns)
p-Bp-	480	<300	350	9	465	11.5	50
o-Bp-	480	450	400	16	610	7.7	27
1-Np-	460	730	385	12	495	8.4	0.86
2-Np-	350	300	420	1.8			
1-Cl-2-Np-	370; 520	800	420; 520	500	440	21	
2-Fl-	490	<300	350	20	440	5.6	
Ph-	520[c]	<300[c]	350[d]	~1[d]	500[c]	12[c]	0.11[c]

[a]In acetonitrile, unless otherwise specified.
[b]In 88% formic acid, unless otherwise specified.
[c]In 100% formic acid.
[d]In pentane.
[e]Bp = biphenylyl; Np = naphthyl; Fl = fluorenyl; Ph = phenyl.

information. This is a complementary tool to ultrafast electronic spectroscopy, particularly important in situations when the electronic spectra of intermediates are not readily observable because they are weak or strongly overlapped. Ultrafast UV–Vis spectroscopy has probed the earliest species produced following photoexcitation of aryl azides as singlet excited azides and nitrenes. The dominant pathway of nitrene decay is ring expansion leading to ketenimine. Both relatively strong IR signals for cyclic ketenimines and its well-defined frequency marker encourage us to explore ultrafast IR studies to probe the ring-extension dynamics.

1.2.2.1 Phenyl Azide. The photochemistry of the phenyl azide, one of the simplest of the aryl azides, has been extensively studied.[9] Photo-induced dissociation leading to molecular nitrogen extrusion is expected to be faster than 1 ps as demonstrated in formic acid. In the dissociation process, singlet phenyl nitrene will be born with an excess of vibrational energy. Thermalized singlet phenyl nitrene isomerizes to benzazirine ($E_a = 5.6$ kcal/mol) which rapidly opens to form 1,2-didehydroazepine (Scheme 1.5).

Nitrene decay has been measured to 0.6 ns post photolysis using picoseconds time-resolved UV–Vis transient absorption spectroscopy.[56] The intermediacy of benzazirine is indicated by calculations, but unfortunately, this is a species with an instantaneous concentration too low to be detected in solution at room temperature. Cyclic ketenimines have been detected by matrix IR spectroscopy and in solution by nanosecond/microsecond time-resolved UV–Vis and IR spectroscopy. These species form in ~1 ns in organic solvents at ambient temperature.

Figure 1.7 presents the time-resolved IR spectra of phenyl azide in the region of 1880 cm^{-1}, where the 1,2-didehydroazepine is known to absorb.[58] The initially observed vibration is broad, but the band sharpens and blue shifts over 10–50 ps. We conclude that the hot singlet nitrene isomerizes to thermally excited ketenimine that

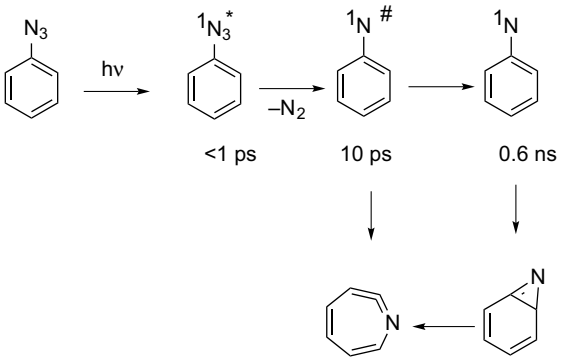

SCHEME 1.5. Reaction pathways for phenyl azide.

then relaxes over 10–50 ps. Since ketenimine rise has also been observed in nanosecond time-resolved experiments, it is clear that these species must be formed in two ways: slowly from the relaxed nitrene (∼0.6 ns) and directly from the hot nitrene (∼10 ps time constant). This latter pathway is a rather rare case in photochemistry, because the energy barrier of the isomerization process is easily overcomed by molecule in a vibrationally excited state (Scheme 1.5).

1.2.2.2 ortho- and para-Biphenylyl Azides. Using ultrafast transient UV–Vis spectroscopy, we have previously reported that ultrafast photolysis of *o*-biphenylyl azide produces a hot singlet nitrene that has a lifetime of 16 ± 3 ps in acetonitrile.[26,27] This nitrene lifetime is shorter than that of singlet *p*-biphenylyl nitrene. This is due to the presence of two competitive isomerization processes leading *o*-biphenylyl

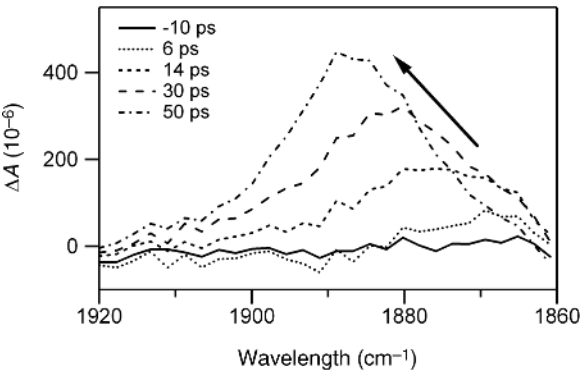

FIGURE 1.7. Time-resolved IR spectra produced on ultrafast photolysis of phenyl azide in chloroform (270 nm excitation). *Source*: Reprinted with permission from the American Chemical Society, *J. Am. Chem. Soc*. 2006, *128*, 14804.

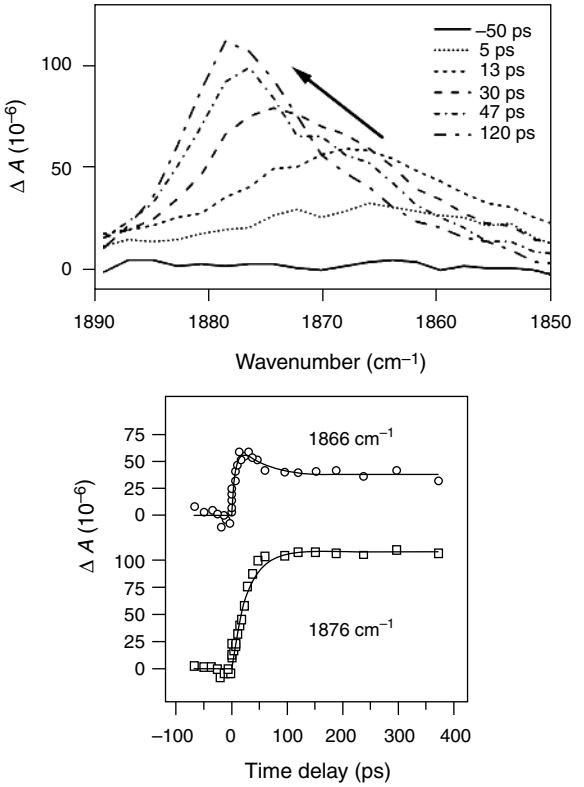

FIGURE 1.8. (a) Time-resolved IR spectra produced on ultrafast photolysis of *ortho*-biphenylyl azide in acetonitrile (270 nm excitation). (b) Selected kinetic traces recorded at 1866 and 1876 cm^{-1}. *Source*: Reprinted with permission from the American Chemical Society, *J. Am. Chem. Soc*. 2006, *128*, 14804.

nitrene to form both isocarbazole and ketenimine. Picosecond IR studies again show the rise of ketenimine. Initially, its absorption band is broad and then sharpens and blue shifts over a 10–50 ps time window (Fig. 1.8a). The ketenimine is formed with a time constant consistent with the decay of the singlet nitrene (∼10 ps, Fig. 1.8b) determined by ultrafast UV–Vis transient absorption spectroscopy.

In contrast to *o*-biphenylyl nitrene, singlet *p*-biphenylyl nitrene does not exhibit any significant population decay on the 100 ps timescale (lifetime is ∼9 ns). Ultrafast UV–Vis studies demonstrated that it is formed thermally excited and undergoes vibrational cooling in 13 ps.[26,27] Attempts to measure the ketenimine formation from *p*-biphenylyl nitrene over a 100 ps time window with IR detection failed. We attribute this to the relatively large rearrangement barrier (6.8 kcal/mol for *p*-biphenylyl nitrene vs. 5.6 kcal/mol for singlet phenyl nitrene), which effectively prohibits isomerization of the corresponding hot nitrene.

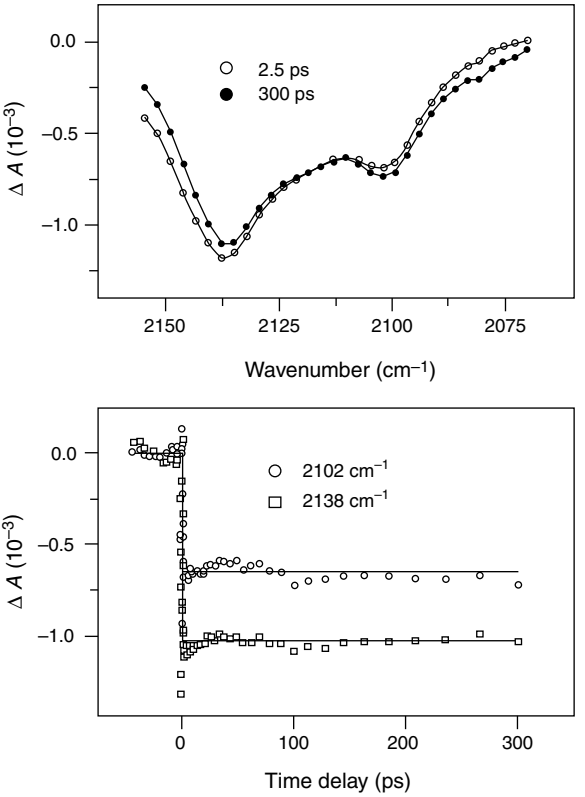

FIGURE 1.9. Time-resolved IR spectra and kinetics produced on ultrafast photolysis of *o*-biphenylyl azide in acetonitrile (270 nm excitation). *Source*: Reprinted with permission from the American Chemical Society, *J. Am. Chem. Soc.* 2006, *128*, 14804.

On UV photoexcitation, azides efficiently form nitrenes by molecular N_2 extrusion. At about 2100 cm^{-1}, there is bleaching of the absorption due to the disappearance of the azide group. Ultrafast IR studies have shown that there is a prompt bleach of the vibrational bands associated with the ground-state azide persisting for $>$300 ps. Representative transient spectra at 2.5 and 300 ps for *o*-biphenylyl azide in acetonitrile are shown in Figure 1.9a, along with the dynamics at 2102 and 2138 cm^{-1} in Figure 1.9b.

1.3 ARYL NITRENIUM IONS

Aryl nitrenium cations and their conjugate bases, aryl nitrenes, are reactive intermediates of fundamental importance.[20–24] Aryl nitrenium cations form covalent adducts with the guanine residues of DNA by a typical electrophilic aromatic

substitution mechanism.[59,60] The formation of these adducts can be correlated with the carcinogenic activity of arylamines.[61,62]

In recent years, the groups of Falvey,[63–68] McClelland,[21–24] and Novak[69–74] have developed convenient precursors for studying the solution phase chemistry of nitrenium cations, which has allowed the measurement of their lifetimes, the determination of their UV–Vis and IR spectra, and the determination of rate constants for reactions with selected nucleophiles, in aqueous solution. The most convenient way to generate mono-substituted nitrenium cations, RNH^+, was developed by McClelland et al. who photolyzed aryl azides in water to generate singlet nitrenes, which are subsequently protonated to form nitrenium cations.[21–24] This method works particularly well when the singlet nitrene to be intercepted has a relatively long lifetime (>10 ns) in aprotic solvent at ambient temperatures. In this manner, *p*-biphenylyl nitrenium cation (*p*-$BpNH^+$), produced by protonation of singlet *p*-biphenylyl nitrene (^{1}*p*-BpN), was readily detected by transient UV–Vis spectroscopy.[21–24] Phillips et al. subsequently studied this nitrenium cation in water using time-resolved resonance Raman spectroscopy and assigned the spectra with the aid of DFT calculations.[25] Similarly, Michalak and Platz produced fluorinated arylnitrenium cations in acidic acetonitrile solution by flash photolysis of the corresponding aryl azides.[75]

The observation of corresponding nitrenium ion spectra for short-lived nitrenes, such as *o*-BpN, 1-NpN, and 2-NpN, were prevented by the very rapid intramolecular cyclization of these nitrenes. However, recently we discovered that aryl nitrenes could be efficiently protonated in formic acid which led us to renewed attempts at interception of *o*-BpN, 1-NpN, and 2-NpN.[76]

Ultrafast spectroscopy is an excellent tool to study proton transfer reactions due to their extremely rapid reaction rates. There are not many reported studies of proton transfer rates between solute and solvent, where the solute acts as proton acceptor and the solvent as proton donor. Apart from singlet nitrenes, this process has been studied for a series of singlet arylcarbenes[29–32,34,35,77] and bipyridine in the singlet excited state[78] (hydrogen atom transfer) in alcohols. Although the reaction is diffusion controlled, the proton transfer rate is not instantaneous (within 100 fs) and is limited by the time needed for solvent reorganization. Our studies of singlet nitrenes in various protic solvents is an attempt to understand the solvent parameters controlling the protonation rate and create a nitrenium cation even in the presence of very competitive deactivation channels (for instance intramolecular rearrangements).

1.3.1 *p*-Biphenylyl Nitrenium Cation

We first studied proton transfer reactions of *p*-biphenylyl azide, *p*-BpN_3 because both the corresponding nitrene[26,27] ^{1}*p*-BpN and the analogous nitrenium cation[21,23] *p*-$BpNH^+$ are well-characterized. Ultrafast laser flash photolysis (270 nm) of *p*-biphenylyl azide (*p*-BpN_3) in a mixture of 50% water and 50% acetonitrile produces the spectra shown in Figure 1.10.[76] A transient absorption band centered at 350 nm, which is assigned to singlet *p*-biphenylyl nitrene ^{1}*p*-BpN, is formed

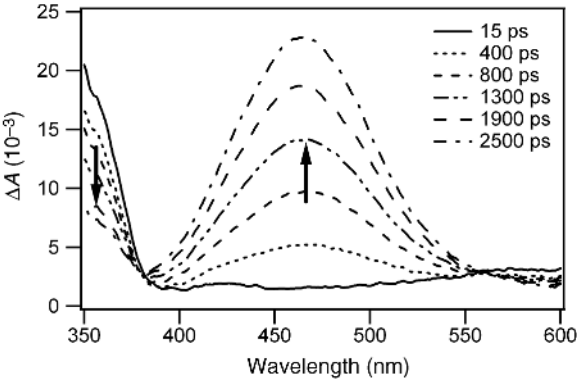

FIGURE 1.10. Transient spectra produced by ultrafast photolysis of *p*-biphenylyl azide in acetonitrile–water (50% vs. 50%) mixture. The spectra were generated by ultrafast LFP (270 nm) with a time window of 15–2500 ps. *Source*: Reprinted with permission from Ref. 84.

within 1 ps. This is in excellent agreement with our previous observation[26,27] of the same nitrene in acetonitrile. As ^{1}*p*-BpN decays, a peak centered at 465 nm is formed, with an isosbestic point at 380 nm. Based on McClelland's work,[21,23] the newly formed 465 nm band is assigned to *p*-biphenylyl nitrenium cation *p*-BpNH$^+$. The rate of formation of the 465 nm band is too slow to be determined accurately with our spectrometer and our best estimation of this time constant is around 3 ns. If the photolysis is performed in 88% formic acid, the decay rate of singlet *p*-biphenylyl nitrene and the formation rate of its corresponding nitrenium cation are identical within experimental error, with a time constant of 11.5 ps. The singlet nitrene decay in 88% formic acid is on the timescale of vibrational cooling of the nitrene in acetonitrile. Thus, it is possible that it is the vibrationally excited, rather than the thermalized singlet nitrene, which undergoes protonation. In 88% formic acid, nitrenium cation *p*-BpNH$^+$ has a lifetime of 50 ns.

McClelland et al. ruled out azide excited states as the precursors of the nitrenium cations based on the fact that the quantum yields of decomposition of the azides remains unchanged over a 20–90% acetonitrile–water mixture, in spite of a decrease in the yield of the nitrenium cations at higher acetonitrile concentration.[23] Consequently, they assigned the singlet nitrene as the precursor of the nitrenium cations. The direct evidence provided in this work[76] confirms that nitrenes are the precursors of nitrenium cations, as first proposed by McClelland group.[21,23]

1.3.2 *o*-Biphenylyl Nitrenium Cation

In acetonitrile, the lifetime of singlet *o*-biphenylyl nitrene ^{1}*o*-BpN is only 16 ps, because ^{1}*o*-BpN is deactivated by the extremely rapid formation of azirine *o*-BpAZ and isocarbazole *o*-BpIC[26,27]. Hence, highly acidic conditions are necessary to produce *o*-BpNH$^+$ in competition with the two intramolecular cyclizations.

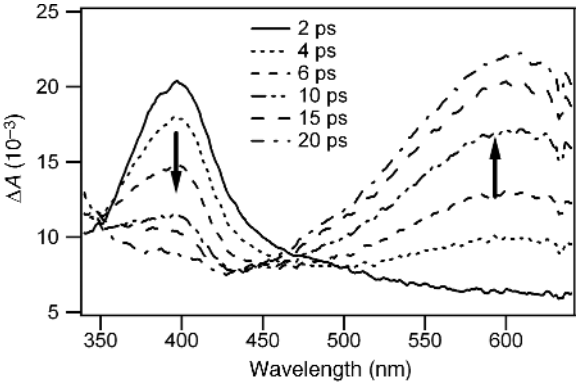

FIGURE 1.11. Transient spectra produced by ultrafast photolysis of *o*-biphenylyl azide in 88% formic acid. The spectra were generated by ultrafast LFP (270 nm) with a time window of 2–20 ps. *Source*: Reprinted with permission from Ref. 84.

Ultrafast photolysis (270 nm) of *o*-biphenylyl azide (*o*-BpN_3) in 88% formic acid produces the spectra in Figure 1.11.[76] A transient absorption band centered at 400 nm is formed within 1 ps, which is assigned to singlet *o*-biphenylyl nitrene (^{1}*o*-BpN), consistent with our previous observation[26,27] of the same nitrene in acetonitrile. As ^{1}*o*-BpN decays, a peak centered at 610 nm is formed, with an isosbestic point at 465 nm. By analogy with the prior example of *p*-BpN_3, the carrier of the 610 nm band is assigned to *o*-biphenylyl nitrenium cation (*o*-$BpNH^+$). This assignment is also consistent with Zhu, Carra, and Bally's study of the same nitrenium ion in Ar-HCl matrices.[76] The singlet nitrene decay in 88% formic acid is also on the timescale of vibrational cooling of the nitrenes in acetonitrile.[26,27] Once again it is the vibrationally excited, rather than the thermalized singlet nitrene, which undergoes protonation.

Global fitting of the decay observed at 400 nm and the growth at 610 nm gives a time constant of 7.7 ps. In acetonitrile, the lifetime of singlet *o*-biphenylyl nitrene is 16 ps, which is mainly deactivated by intramolecular cyclization to azirine *o*-BpAZ and isocarbazole *o*-BpIC. Assuming that the intramolecular decay processes of ^{1}*o*-BpN have the same rate constants in 88% formic acid as in acetonitrile, we deduce that the apparent protonation rate constant is $6.7 \times 10^{10}\,s^{-1}$ in 88% formic acid. Based on this assumption, we can also conclude that 52% of ^{1}*o*-BpN is protonated in this acidic solvent. The carrier of the 610 nm band shows only very little decay in a 3 ns time window. Its lifetime of 27 ns in 88% formic acid was determined by nanosecond time-resolved LFP techniques.

1.3.3 1-Naphthyl Nitrenium Cation

Ultrafast photolysis ($\lambda_{ex} = 270$ nm) of 1-naphthyl azide (1-NpN_3) in 88% formic acid produces the spectra shown in Figure 1.12.[76] A peak centered at 380 nm is formed

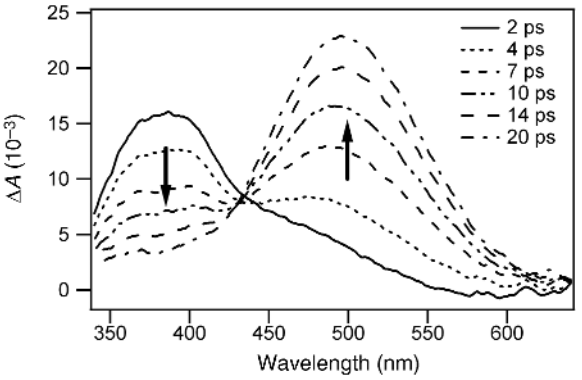

FIGURE 1.12. Transient spectra produced by ultrafast photolysis of 1-naphthyl azide in 88% formic acid. The spectra were generated by ultrafast LFP (270 nm) with a time window of 2–20 ps. *Source*: Reprinted with permission from Ref. 84.

within 1 ps of the laser pulse. The carrier of this absorption band is assigned to singlet 1-naphthyl nitrene (^{1}1-NpN), consistent with its previous observation[26] in acetonitrile. As ^{1}1-NpN decays, a new species is formed, with an absorption centered at 495 nm and an isosbestic point at 430 nm. The carrier of the 495 nm absorption band is assigned to 1-naphthyl nitrenium cation (1-NpNH$^+$). This is consistent with Kung and Falvey's report of the spectrum of the closely related species *N*-methyl-*N*-1-naphthyl nitrenium cation.[66] This assignment is also consistent with CASPT2 calculations and low temperature studies of the same nitrenium ion in Ar–HCl matrices.[76] Thus, we have little doubt that this assignment is correct.

Global fitting of the decay at 380 nm and the growth at 495 nm give a time constant of 8.4 ps. In acetonitrile, the lifetime of singlet 1-naphthyl nitrene (12 ps) is mainly limited by intramolecular cyclization to form azirine 1-NpAZ. If we make the same assumption as in the case of *o*-biphenylyl azide, that the formation of the azirine has the same rate constant in 88% formic acid as in acetonitrile, then the apparent protonation rate constant is $3.6 \times 10^{10}\,s^{-1}$ in 88% formic acid. Therefore, we can also conclude that 30% of the singlet 1-naphthyl nitrene produced under these conditions is protonated in this solvent. As before, it is the vibrationally excited, rather than the thermalized singlet nitrene, which undergoes protonation. The lifetime of 1-naphthyl nitrenium cation is only 860 ps, which explains why this species cannot be observed by nanosecond time-resolved LFP methods.

1.3.4 2-Naphthyl Nitrenium Cation

Singlet 2-naphthyl nitrene ^{1}2-NpN is the shortest-lived nitrene discovered to date ($\tau = 1.8$ ps). The apparent rate constant of intramolecular reactions for ^{1}2-NpN is $5.6 \times 10^{11}\,s^{-1}$. Based on our analysis in Sections 1.3.2 and 1.3.3, the apparent protonation rate constants for ^{1}*o*-BpN and ^{1}1-NpN are $6.7 \times 10^{10}\,s^{-1}$ and

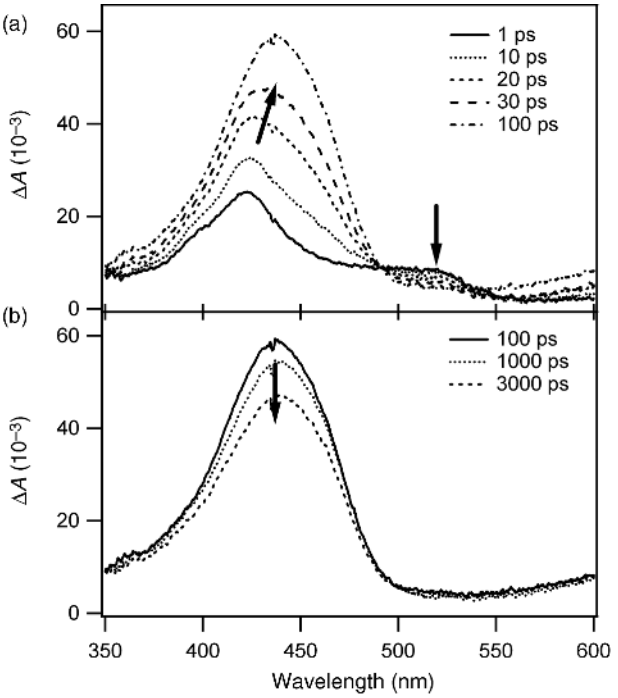

FIGURE 1.13. Transient absorption spectra were produced by 308 nm photolysis of 1-chloro-2-naphthyl azide in 88% formic acid at ambient temperature. The transient spectra were recorded in time windows of (a) 1–100 ps and (b) 100–3000 ps. Unpublished results.

$3.6 \times 10^{10}\,s^{-1}$ in 88% formic acid, respectively. These values are around one order of magnitude smaller than the apparent rate constant of intramolecular reactions for ^{1}2-NpN in acetonitrile. Thus, it is not surprising that a similar ultrafast photolysis of 2-NpN$_3$ in 88% formic acid cannot produce a measurable amount of the corresponding nitrenium ion (unpublished results).

To avoid the fast intramolecular reactions of ^{1}2-NpN, the same strategy described in Section 1.2.1.2 was applied to study the nitrenium ion of 2-NpN (Scheme 1.4). Ultrafast photolysis ($\lambda_{ex} = 308$ nm) of 1-chloro-2-naphthyl azide (Cl-2-NpN$_3$) in 88% formic acid produces the transient spectrum shown in Figure 1.13. The spectrum recorded 1 ps after the laser pulse (Fig. 1.13a), centered at 425 nm with a shoulder at 520 nm, can be confidently assigned to ^{1}2-NpN based on the discussion in Section 1.2.1.2. As the spectra evolve between 1 and 100 ps, the 425 nm band shifts to 440 nm and the 520 nm shoulder band decays to the baseline (Fig. 1.13a). The growth time constant of the 440 nm band and the decay time constant of 520 nm band are the same within experimental error ($\tau = 21 \pm 5$ ps). This newly formed 440 nm band is assigned to the corresponding nitrenium ion for ^{1}Cl-2-NpN. Carra and Bally predicted that the UV spectrum of 2-NpNH$^+$ absorbs at 381 and 357 nm, which is in fair agreement with the experimental absorption of Cl-2-NpNH$^+$.

1.3.5 Phenyl Nitrenium Cation

Although product studies indicate that parent singlet phenyl nitrene ($\tau \approx 1$ ns, organic solvents) can be protonated in acidic aqueous solution, nanosecond time-resolved laser flash photolysis studies failed to produce the transient spectrum of phenyl nitrenium cation ($PhNH^+$).[23,79] This simplest arylnitrenium cation $PhNH^+$ has been investigated theoretically. Using density functional theory (DFT), Cramer et al. predicts that parent phenyl nitrenium cation has a singlet ground state that is favored by 21.2 kcal/mol over the lowest-energy triplet state.[80] In addition, a number of substituted arylnitrenium cations have been studied by LFP techniques with nanosecond time-resolved UV–Vis,[21–24,63–66] IR,[67,68] and Raman[25,81,82] spectroscopy. However, to our knowledge, spectroscopic features of the parent system $PhNH^+$ remain elusive. McClelland estimated the lifetime of $PhNH^+$ is 125–240 ps in aqueous solution based on an azide trapping experiment.[79] The time resolution of a conventional ns-LFP system is not sufficient to observe such a short-lived reactive intermediate. Thus, ultrafast time-resolved spectroscopy was required to study phenyl nitrenium cation in solution.

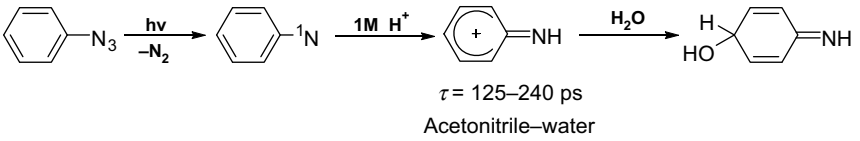

Ultrafast photolysis of phenyl azide (PhN_3) in 100% formic acid with a 300 fs pulse of 308 nm light results in the spectral changes shown in Figure 1.14, where artifacts due to solvent two photo absorption have been subtracted.[57] A broad transient absorption, centered at 520 nm, is detected at the earliest times observable (Fig. 1.14a). As discussed in Section 1.2.1.3, the broad transient absorption is assigned to an excited state of phenyl azide ($^1PhN_3^*$).

In 100% formic acid, $^1PhN_3^*$ decays within our instrument response function (300 fs) and a growth in absorption below 400 nm is observed, which is assigned to singlet phenyl nitrene (^1PhN). This assignment is consistent with the singlet nitrene spectrum reported previously.[56,83] Subsequently, the decay ($\tau = 12.0 \pm 1.0$ ps) of ^1PhN is accompanied by the growth of transient absorption centered at 500 nm (Fig. 1.14b). Within experimental error, the time constant of the decay recorded at 360 nm is the same as that of the growth of transient absorption monitored at 500 nm.

In nonacidic solutions such as ACN, the decay of ^1PhN is not accompanied by the formation of a transient species absorbing at 500 nm.[56,83] Following our study of the efficient protonation of *o*-biphenylyl and 1-naphthyl nitrene to form the corresponding nitrenium ions in 88% formic acid,[84] the transient absorption at 500 nm is assigned to phenyl nitrenium ion ($PhNH^+$). Falvey's group studied a related species, *N*-methyl-*N*-tolylnitrenium ion *p*-$MePhNMe^+$, which has a strong absorption band centered at 325 nm and a weak absorption tail in the visible region centered around 470 nm.[85] The weak band of *p*-$MePhNMe^+$ has absorption similar to that observed for $PhNH^+$. TD-DFT calculations predict that the parent system $PhNH^+$ has two

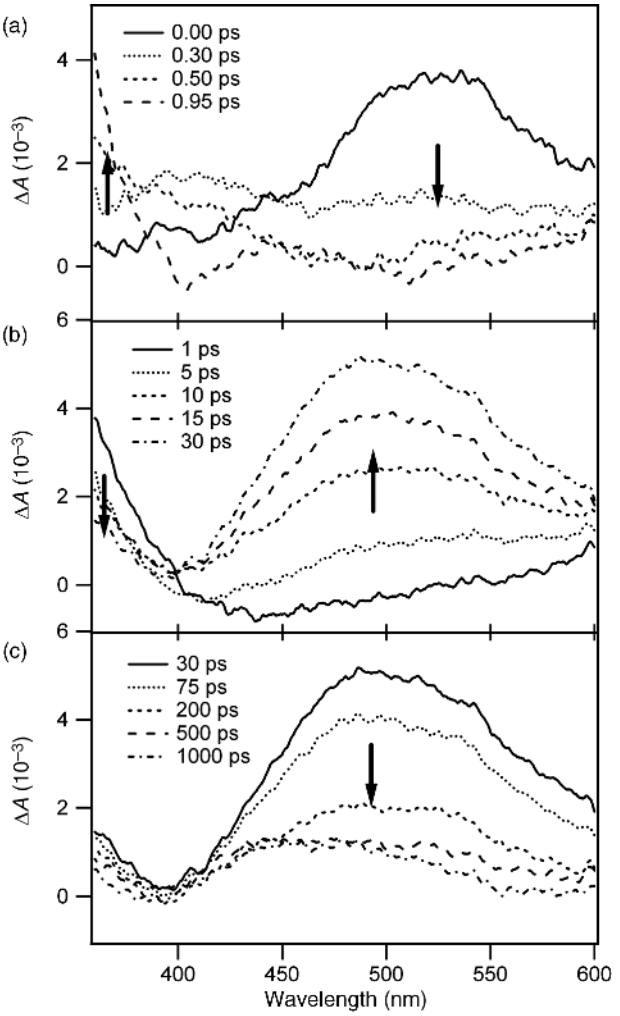

FIGURE 1.14. Transient spectra generated by ultrafast LFP (308 nm) of phenyl azide in 100% formic acid with time windows (a) 0–0.95 ps, (b) 1–30 ps, and (c) 30–1000 ps. *Source*: Reprinted with permission from Ref. 57.

$\pi \rightarrow \pi^*$ transitions at 259 nm ($f = 0.2429$) and 450 nm ($f = 0.0284$), respectively, which is in fair agreement with the experimental results. Based on these calculations, the known spectrum of *N*-methyl-*p*-tolylnitrenium ion, and the absence of the 500 nm absorbing transient in ACN, the assignment of the 500 nm band to $PhNH^+$ appears secure.

The lifetime of $PhNH^+$ is 110 ± 14 ps in 100% formic acid, which is in excellent agreement with the value estimated by Fishbein and McClelland in aqueous solution.[79]

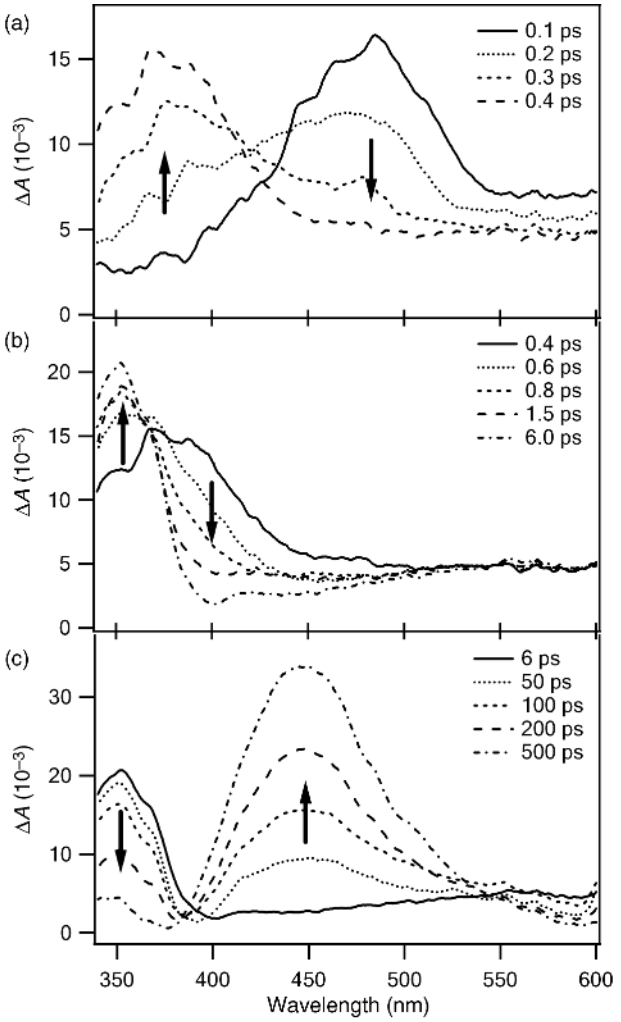

FIGURE 1.15. The transient spectra were generated by ultrafast LFP (270 nm) of 2-fluorenyl azide (FlN_3) in methanol with time windows (a) 0.1–0.4 ps, (b) 0.4–6 ps, and (c) 6–500 ps. *Source*: Reprinted with permission from Ref. 41.

1.3.6 2-Fluorenyl Nitrenium Cation and the Influence of Solvent

Ultrafast photolysis[26] ($\lambda_{ex} = 270$ nm) of 2-fluorenyl azide (FlN_3) in methanol produces the spectra of Figure 1.15.[41] A band centered at 490 nm is formed within the instrument response (300 fs), which can be assigned to a singlet excited state of the azide ($^1FlN_3^*$), based on our previous studies.[26] As $^1FlN_3^*$ decays, a new band is formed, centered at 380 nm which blue shifts to 350 nm over 6 ps. The carrier of this

newly formed band is assigned to singlet 2-fluorenyl nitrene (^{1}FlN). The blue shift and band narrowing processes are typical of vibrational cooling[26] (Fig. 1.15b). Subsequently, ^{1}FlN decays and a 450 nm band is formed, which is assigned to 2-fluorenyl nitrenium ion ($FlNH^+$). This assignment is in excellent agreement with McClelland's observation of the same nitrenium ion in acetonitrile–water using nanosecond time-resolved laser flash photolysis techniques.[21,23,24] The decay of ^{1}FlN and the growth of $FlNH^+$ share the same time constant (250 ps) in methanol within experimental error. In methanol-OD, the time constant of the decay of ^{1}FlN and the growth of $FlNH^+$ lengthen to 380 ps, showing a kinetic isotope effect of 1.5. This relatively small primary isotope effect is not surprising as it is similar to the values observed in the protonation of singlet aryl carbenes.[77] Ultrafast photolysis of FlN_3 in acetonitrile, a nonacidic solvent, produces the broad 490 nm band of $^1FlN_3^*$ and the 350 nm band of ^{1}FlN. However, the 450 nm band was not observed in the aprotic solvent. Based on the known spectrum of $FlNH^+$, the absence of the 450 nm absorbing transient in acetonitrile, and the kinetic isotope effect, the assignment of the 450 nm band to $FlNH^+$ is secure.

The effect of solvent on the rates of nitrenium ion formation was studied in a series of protic solvents. In the eight solvents utilized in this study, the protonation time constant (τ) of ^{1}FlN is shortest in formic acid (10.5 ps) and slowest in formamide (1290 ps). The intersystem crossing rate of ^{1}FlN is 20 ns in acetonitrile. Assuming that the ISC rates in the eight solvents employed in this study are similar to that in acetonitrile, we can conclude that the decay of the nitrene will be largely controlled by protonation, which is at least 20 times faster than ISC.

Simple correlations of $\log k_p$ with solvent physical properties such as dielectric constant and refractive index were not found, where k_p is the apparent protonation rate constant and equals to $1/\tau$. We also considered empirical solvent parameters. Dimroth's $E_T(30)$ parameters[86,87] provide a widely used scale to evaluate solvent polarity. In this case, however, the correlation between $\log k_p$ and $E_T(30)$ is also scattered. A traditional Brønsted plot ($\log k_p$ vs. pK_a) was not linear. The acidity of a particular organic solute in water does not correlate with the rate of nitrene protonation in the bulk organic solvent! An apparent violation is that $\log k_p$ is greater in trifluoroethanol TFE than in acetic acid. However, the pK_a for acetic acid is smaller than that of TFE. As pK_a is a scale for molecular properties, it is clear that in this case, it is inappropriate to use molecular properties in water or dimethyl sulfoxide DMSO to evaluate bulk solvent properties.

Kamlet, Abboud, and Taft (KAT) developed the solvatochromic solvent parameters α and β to describe solvent hydrogen bonding donor (HBD) and hydrogen bonding acceptor (HBA) abilities.[88] A better HBD solvent deprotonates more easily. Our data show a fair correlation with the α parameters. Subsequently, Swain et al. coined the terms *Acidity* and *Basicity* to describe a set of new parameters to measure the acid–base properties of bulk solvents[89] using the equation $aA + bB + c$, where A and B depend only on solvent and a, b, and c depend on the reaction. The parameter A refers to the anion-solvating tendency and B refers to the cation-solvating tendency of the solvent. The authors fitted the free energy changes due to solvent using 1080 data sets for 61 solvents and 77 solvent-sensitive reactions and physicochemical

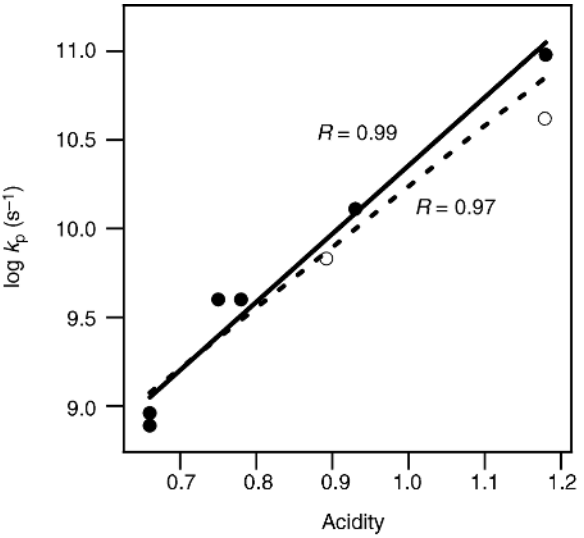

FIGURE 1.16. The correlation of log k_p with Swain's acidity parameters. The acidity parameters for formic acid, acetic acid, methanol, ethanol, ethylene glycol and formamide (solid circles) are obtained from Swain's paper.[89] The acidity parameters for 2,2,2-trifluoroethanol and propionic acid (open circles) are calculated from KAT's parameters.[90] The dashed line is the best-fit linear correlation of the data for all eight solvents of this study ($R = 0.97$). The solid line is the linear correlation of the data for the six solvents excluding 2,2,2-trifluoroethanol and propionic acid ($R = 0.99$). *Source*: Reprinted with permission from Ref. 41.

properties, taken from the literature, such as reaction rate constants, equilibrium constants, product ratios, and UV–Vis, IR, and NMR spectra. They found that A and B can describe solvent hydrogen-bond donating and accepting abilities and proposed that these parameters could be used to evaluate *bulk* solvent acidity and basicity. To a first-order approximation, the rate of nitrene protonation $= k_{H+}[H^+][^1FlN] = k_p[^1FlN]$, where k_{H+} is the bimolecular rate constant for the reaction between ^1FlN and protons, $[H^+]$ and $[^1FlN]$ are the proton and 2-fluorenyl nitrene concentrations in the solvent. It is of course possible that the nitrene reacts with the solvent molecule directly to achieve proton transfer from solvent to solute. This measure of proton-donating ability also correlates with acidity values. Thus, the nitrene protonation rate can, in principle, correlate with the acidity of bulk solvent, as quantified by the acidity scale.

Excluding TFE and propionic acid, six of the eight solvents used in this study have known Swain acidity parameters.[89] The correlation of log k_p with the six solvent acidities is excellent ($R = 0.99$, the solid line of Fig. 1.16). Stimulated by the similarity between the KAT and Swain's parameters, Marcus found a relationship between these two sets of solvent empirical parameters,[90] which is that acidity $= 0.03 + 0.64\ \alpha + 0.25\ \pi^*$ and basicity $= 0.04 + 0.035\ \beta + 0.94\ \pi^*$ (exclude acetic

acid). The two missing Swain parameters of 2,2,2-trifluoroethanol and propionic acid were calculated accordingly based on the Marcus relationships.[90] Including the two calculated acidity parameters, the correlation of log k_p with solvent acidities remains excellent ($R = 0.97$, the dashed line of Fig. 1.16).

Multilinear regression analysis has been performed on these data following Swain's equation $\log k_p = a \times \text{acidity} + b \times \text{basicity} + c$. When we consider six solvents (excluding 2,2,2-trifluoroethanol and propionic acid) or on consideration of all eight solvents, a multilinear regression analysis has a high correlation coefficient. The absolute value of the fitting coefficient a is found to be more than ten times greater than b. This demonstrates that the ability of a bulk solvent to solvate the conjugate anion produced in a proton transfer reaction is the dominant effect on nitrene protonation.

In summary, the rate of protonation of a nitrene in an organic solvent does not correlate with the acidity of the solvent when that solvent is a solute in water, nor does it correlate with other simple parameters such as dielectric constant or $E_T(30)$ parameters. The rate protonation of singlet aryl nitrenes do correlate with Swain's acidity parameters. The Swain scale and the rate of nitrene protonation provide a convenient way to measure the bulk acidities of neat organic solvents.

1.4 CONCLUSIONS

Ultrafast time-resolved UV–Vis spectroscopic methods can be used to detect the absorption spectra of aromatic azides. These excited states typically have lifetimes of less than 300 fs. Theoretical analyses discussed in an accompanying chapter indicate that we have detected S_2 states of the aryl azides. These states are bound because the excitation is localized on the aromatic ring or rings. The S_2 states relax to S_1 states (not detectable) which rapidly fragment to form singlet nitrenes and molecular nitrogen.

The singlet nitrenes are born with excess vibrational energy that transferred to solvent over 10–20 ps. This is manifest by a narrowing of the absorption maxima. Certain singlet nitrenes (*ortho*-biphenyl, 1- and 2-naphthyl) are in very shallow potential minima and isomerize as fast or faster than they shed heat to solvent.

Ultrafast time-resolved infrared spectroscopy reveals that vibrationally excited singlet nitrenes both isomerize (1–20 ps) to vibrationally excited 1,2-didehydroazepines and relax to thermalized singlet nitrenes. The latter species isomerize to cool 1,2-didehydroazepines over hundreds to thousands of picoseconds. A ketenimine is formed with an $\sim$10 ps time constant from *hot o*-biphenylyl and phenyl nitrenes. In the latter case, there is a second slower component ($\sim$1 ns). This slow process is when vibrationally relaxed *cold* phenyl nitrene overcomes the energy barrier in the ring-expansion process. The energy barrier for *p*-biphenylyl nitrene is so high, that hot nitrene does not form ketenimine. In future studies, we will determine the percentage of ketenimine formed in the picosecond and nanosecond pathways as a function of pump wavelength, solvent, and nitrene structure. In formic acid, singlet nitrenes are efficiently protonated to form nitrenium cations.

ACKNOWLEDGMENTS

The support of the US National Science Foundation over several decades is gratefully acknowledged. MSP wishes to thank his many students, mentioned in the references, for their hardwork, excellent laboratory skills, and dedication to the project. Special thanks go as well to Professor Terry Gustafson whose vision led to the Center for Chemical and Biophysical Dynamics, where most of this work was performed, to Professor Christopher Hadad who provided numerous useful computational-derived insights and Professor Nina Gritsan whose work on the nanosecond timescale allowed us to interpret the ultrafast time-resolved data.

REFERENCES

1. Kasha, M. *Discuss. Faraday Soc.* **1950**, *9*, 14–19.
2. Lakowicz, J. R. *Principles of Fluorescence Spectroscopy*, 2nd ed., Kluwer Academic/ Plenum Publishers, New York, **1999**.
3. Woggon, U.; Giessen, H.; Gindele, F.; Wind, O.; Fluegel, B.; Peyghambarian, N. *Phys. Rev. B Condens. Matter* **1996**, *54*, 17681–17690.
4. Beer, M.; Longuet-Higgins, H. C. *J. Phys. Chem.* **1955**, *23*, 1390–1391.
5. Bogdanova, A.; Popik, V. V. *J. Am. Chem. Soc.* **2003**, *125*, 14153–14162.
6. Bogdanova, A.; Popik, V. V. *J. Am. Chem. Soc.* **2003**, *125*, 1456–1457.
7. Lwowski, W., Ed., *Nitrenes*, Wiley, New York, **1970**.
8. Scriven, E. F. V. *Azides and Nitrenes: Reactivity and Utility*, Academic Press, New York, **1984**.
9. Gritsan, N. P.; Platz, M. S. *Chem. Rev. (Washington, DC, United States)* **2006**, *106*, 3844–3867.
10. Platz, M. S. Nitrenes. Moss, R. A., Platz, M. S., Jones, M. Jr., Eds., in *Reactive Intermediates Chemistry*, Wiley, New York, **2004**, pp. 501–560.
11. Koryttsev, K. Z.; Oleinik, A. V.; Korshuniv, I. A. *Tr. Khim. Khim. Tekhnol.* **1971**, 207–211.
12. Koryttsev, K. Z.; Oleinik, A. V. *Zh. Fiz. Khim.* **1973**, *47*, 700.
13. Geiger, M. W.; Elliot, M. M.; Karacostas, V. D.; Moricone, T. J.; Salmon, J. B.; Sideli, V. L.; St. Onge, M. A. *Photochem. Photobiol.* **1984**, *40*, 545–548.
14. Jenkins, R. F.; Waddell, W. H.; Richter, H. W. *J. Am. Chem. Soc.* **1987**, *109*, 1583–1584.
15. Budyka, M. F.; Kantor, M. M.; Alfimov, M. V. *Izv. Akad. Nauk, Ser. Khim.* **1992**, 752–754.
16. Budyka, M. F.; Kantor, M. M.; Alfimov, M. V. *Usp. Khim.* **1992**, *61*, 48–74.
17. Avramenko, L. F.; Eshchenko, N. P.; Kondratenko, P. A.; Novikova, E. A.; Syromyatnikov, V. G. *Ukr. Khim. Zh. (Russ. Ed.)* **2005**, *71*, 64–70.
18. Budyka, M. F.; Biktimirova, N. V.; Gavrishova, T. N.; Laukhina, O. D. *Russ. J. Phys. Chem.* **2005**, *79*, 1666–1671.
19. Zhu, Z.; Bally, T.; Stracener, L. L.; McMahon, R. J. *J. Am. Chem. Soc.* **1999**, *121*, 2863–2874.

20. Falvey, D. E. Nitrenium ions. Moss, R. A., Platz, M. S., Jones, M., Eds., in *Reactive Intermediate Chemistry*, Wiley, Hoboken, NJ, **2004**, pp. 593–650.
21. Mcclelland, R. A.; Davidse, P. A.; Hadzialic, G. *J. Am. Chem. Soc.* **1995**, *117*, 4173–4174.
22. McClelland, R. A. *Tetrahedron* **1996**, *52*, 6823–6858.
23. McClelland, R. A.; Kahley, M. J.; Davidse, P. A.; Hadzialic, G. *J. Am. Chem. Soc.* **1996**, *118*, 4794–4803.
24. Davidse, P. A.; Kahley, M. J.; McClelland, R. A.; Novak, M. *J. Am. Chem. Soc.* **1994**, *116*, 4513–4514.
25. Zhu, P.; Ong, S. Y.; Chan, P. Y.; Poon, Y. F.; Leung, K. H.; Phillips, D. L. *Chem. Eur. J.* **2001**, *7*, 4928–4936.
26. Burdzinski, G.; Hackett, J. C.; Wang, J.; Gustafson, T. L.; Hadad, C. M.; Platz, M. S. *J. Am. Chem. Soc.* **2006**, *128*, 13402–13411.
27. Burdzinski, G. T.; Gustafson, T. L.; Hackett, J. C.; Hadad, C. M.; Platz, M. S. *J. Am. Chem. Soc.* **2005**, *127*, 13764–13765.
28. Tsao, M.-L.; Gritsan, N.; James, T. R.; Platz, M. S.; Hrovat, D. A.; Borden, W. T. *J. Am. Chem. Soc.* **2003**, *125*, 9343–9358.
29. Wang, J.; Burdzinski, G.; Gustafson, T. L.; Platz, M. S. *J. Org. Chem.* **2006**, *71*, 6221–6228.
30. Wang, J.; Burdzinski, G.; Gustafson, T. L.; Platz, M. S. *J. Am. Chem. Soc.* **2007**, *129*, 2597–2606.
31. Wang, J.; Kubicki, J.; Hilinski, E. F.; Mecklenburg, S. L.; Gustafson, T. L.; Platz, M. S. *J. Am. Chem. Soc.* **2007**, *129*, 13683–13690.
32. Burdzinski, G. T.; Wang, J.; Gustafson, T. L.; Platz, M. S. *J. Am. Chem. Soc.* **2008**, *130*, 3746–3747.
33. Wang, J.; Burdzinski, G.; Kubicki, J.; Gustafson, T. L.; Platz, M. S. *J. Am. Chem. Soc.* **2008**, *130*, 5418–5419.
34. Wang, J.; Kubicki, J.; Gustafson, T. L.; Platz, M. S. *J. Am. Chem. Soc.* **2008**, *130*, 2304–2313.
35. Wang, J.; Zhang, Y.; Kubicki, J.; Platz, M. S. *Photochem. Photobiol. Sci.* **2008**, *7*, 552–557.
36. Laermer, F.; Elsaesser, T.; Kaiser, W. *Chem. Phys. Lett.* **1989**, *156*, 381–386.
37. Elsaesser, T.; Kaiser, W. *Annu. Rev. Phys. Chem.* **1991**, *42*, 83–107.
38. Miyasaka, H.; Hagihara, M.; Okada, T.; Mataga, N. *Chem. Phys. Lett.* **1992**, *188*, 259–264.
39. Schwarzer, D.; Troe, J.; Votsmeier, M.; Zerezke, M. *J. Phys. Chem.* **1996**, *105*, 3121–3131.
40. Gritsan, N. P.; Polshakov, D. A.; Tsao, M.-L.; Platz, M. S. *Photochem. Photobiol. Sci.* **2005**, *4*, 23–32.
41. Wang, J.; Burdzinski, G.; Platz, M. S. *Org. Lett.* **2007**, *9*, 5211–5214.
42. Sundberg, R. J.; Brenner, M.; Suter, S. R.; Das, B. P. *Tetrahedron Lett*. **1970**, 2715–2718.
43. Sundberg, R. J.; Heintzelman, R. W. *J. Org. Chem.* **1974**, *39*, 2546–2552.
44. Hilton, S. E.; Scriven, E. F. V.; Suschitzky, H. *J. Chem. Soc., Chem. Commun.* **1974**, 853–854.
45. Carroll, S. E.; Nay, B.; Scriven, E. F. V.; Suschitzky, H. *Synthesis* **1975**, 710–711.

46. Carroll, S. E.; Nay, B.; Scriven, E. F. V.; Suschitzky, H. *Tetrahedron Lett*. **1977**, 943–946.
47. Carroll, S. E.; Nay, B.; Scriven, E. F. V.; Suschitzky, H.; Thomas, D. R. *Tetrahedron Lett*. **1977**, 3175–3178.
48. Nay, B.; Scriven, E. F. V.; Suschitzky, H.; Khan, Z. U. *Synthesis* **1977**, 757–758.
49. Leyva, E.; Platz, M. S. *Tetrahedron Lett*. **1987**, *28*, 11–14.
50. Dunkin, I. R.; Thomson, P. C. P. *J. Chem. Soc., Chem. Commun.* **1980**, 499–501.
51. Schrock, A. K.; Schuster, G. B. *J. Am. Chem. Soc.* **1984**, *106*, 5234–5240.
52. Maltsev, A.; Bally, T.; Tsao, M.-L.; Platz, M. S.; Kuhn, A.; Vosswinkel, M.; Wentrup, C. *J. Am. Chem. Soc.* **2004**, *126*, 237–249.
53. Tsao, M.-L.; Platz, M. S. *J. Phys. Chem. A* **2004**, *108*, 1169–1176.
54. Wang, J.; Kubicki, J.; Burdzinski, G.; Hackett, J. C.; Gustafson, T. L.; Hadad, C. M.; Platz, M. S. *J. Org. Chem.* **2007**, *72*, 7581–7586.
55. Tsao, M.-L.; Platz, M. S. *J. Am. Chem. Soc.* **2003**, *125*, 12014–12025.
56. Born, R.; Burda, C.; Senn, P.; Wirz, J. *J. Am. Chem. Soc.* **1997**, *119*, 5061–5062.
57. Wang, J.; Kubicki, J.; Platz, M. S. *Org. Lett.* **2007**, *9*, 3973–3976.
58. Li, Y. Z.; Kirby, J. P.; George, M. W.; Poliakoff, M.; Schuster, G. B. *J. Am. Chem. Soc.* **1988**, *110*, 8092–8098.
59. Cheng, B.; McClelland, R. A. *Can. J. Chem.* **2001**, *79*, 1881–1886.
60. McClelland, R. A.; Ahmad, A.; Dicks, A. P.; Licence, V. E. *J. Am. Chem. Soc.* **1999**, *121*, 3303–3310.
61. Miller, E. C. *Cancer Res*. **1978**, *38*, 1479–1496.
62. Miller, J. A. *Cancer Res*. **1970**, *30*, 559–576.
63. Anderson, G. B.; Falvey, D. E. *J. Am. Chem. Soc.* **1993**, *115*, 9870–9871.
64. Robbins, R. J.; Yang, L. L. N.; Anderson, G. B.; Falvey, D. E. *J. Am. Chem. Soc.* **1995**, *117*, 6544–6552.
65. Srivastava, S.; Falvey, D. E. *J. Am. Chem. Soc.* **1995**, *117*, 10186–10193.
66. Kung, A. C.; Falvey, D. E. *J. Org. Chem.* **2005**, *70*, 3127–3132.
67. Srivastava, S.; Ruane, P. H.; Toscano, J. P.; Sullivan, M. B.; Cramer, C. J.; Chiapperino, D.; Reed, E. C.; Falvey, D. E. *J. Am. Chem. Soc.* **2000**, *122*, 8271–8278.
68. Srivastava, S.; Toscano, J. P.; Moran, R. J.; Falvey, D. E. *J. Am. Chem. Soc.* **1997**, *119*, 11552–11553.
69. Novak, M.; Kahley, M. J.; Eiger, E.; Helmick, J. S.; Peters, H. E. *J. Am. Chem. Soc.* **1993**, *115*, 9453–9460.
70. Novak, M.; Kahley, M. J.; Lin, J.; Kennedy, S. A.; Swanegan, L. A. *J. Am. Chem. Soc.* **1994**, *116*, 11626–11627.
71. Novak, M.; Kennedy, S. A. *J. Am. Chem. Soc.* **1995**, *117*, 574–575.
72. Novak, M.; Kazerani, S. *J. Am. Chem. Soc.* **2000**, *122*, 3606–3616.
73. Novak, M.; Rajagopal, S. *Adv. Phys. Org. Chem.* **2001**, *36*, 167–254.
74. Novak, M.; Rajagopal, S. *Chem. Res. Toxicol.* **2002**, *15*, 1495–1503.
75. Michalak, J.; Zhai, H. B.; Platz, M. S. *J. Phys. Chem.* **1996**, *100*, 14028–14036.
76. Wang, J.; Burdzinski, G.; Zhu, Z.; Platz, M. S.; Carra, C.; Bally, T. *J. Am. Chem. Soc.* **2007**, *129*, 8380–8388.
77. Peon, J.; Polshakov, D.; Kohler, B. *J. Am. Chem. Soc.* **2002**, *124*, 6428–6438.

78. Didierjean, C.; Buntinx, G.; Poizat, O. *J. Phys. Chem. A* **1998**, *102*, 7938–7944.
79. Fishbein, J. C.; McClelland, R. A. *Can. J. Chem.* **1996**, *74*, 1321–1328.
80. Cramer, C. J.; Dulles, F. J.; Falvey, D. E. *J. Am. Chem. Soc.* **1994**, *116*, 9787–9788.
81. Zhu, P.; Ong, S. Y.; Chan, P. Y.; Leung, K. H.; Phillips, D. L. *J. Am. Chem. Soc.* **2001**, *123*, 2645–2649.
82. Chan, P. Y.; Ong, S. Y.; Zhu, P.; Zhao, C.; Phillips, D. L. *J. Phys. Chem. A* **2003**, *107*, 8067–8074.
83. Gritsan, N. P.; Yuzawa, T.; Platz, M. S. *J. Am. Chem. Soc.* **1997**, *119*, 5059–5060.
84. Wang, J.; Burdzinski, G.; Zhu, Z.; Platz, M. S.; Carra, C.; Bally, T. *J. Am. Chem. Soc.* **2007**, *129*, 8380–8388.
85. Kung, A. C.; Chiapperino, D.; Falvey, D. E. *Photochem. Photobiol. Sci.* **2003**, *2*, 1205–1208.
86. Dimroth, K.; Reichardt, C.; Siepmann, T.; Bohlmann, F. *Justus Liebigs Ann. Chem.* **1963**, *661*, 1–37.
87. Reichardt, C. *Chem. Rev. (Washington, DC, United States)* **1994**, *94*, 2319–2358.
88. Kamlet, M. J.; Abboud, J. L.; Taft, R. W. *J. Am. Chem. Soc.* **1977**, *99*, 6027–6038.
89. Swain, C. G.; Swain, M. S.; Powell, A. L.; Alunni, S. *J. Am. Chem. Soc.* **1983**, *105*, 502–513.
90. Marcus, Y. *Chem. Soc. Rev.* **1993**, *22*, 409–416.